Int. J. Heat Mass Transfer. Vol. 20. pp. 207 214. Pergamon Press 1977. Printed in Great Britain

MEASUREMENTS OF FORCED CONVECTIVE HEAT TRANSFER TO SUPERCRITICAL HELIUM

D. J. BRASSINGTON and D. N. H. CAIRNS
Central Electricity Research Laboratories, Leatherhead, England

(*Received* 2 *December* 1975 *and in revised form* 8 *July* 1976)

Abstract—The heat-transfer coefficient of supercritical helium flowing both up and down an 18 mm i.d. vertical tube has been measured. The conditions covered were 4.4–15 K, 2.2–14 bars, with heat fluxes up to 2500 W/m^2 and Reynolds numbers between 5×10^4 and 10^6. The results can be represented with standard deviations of $\sim 12\%$ by $Nu = cRe^{0.8}Pr^{0.4}$ where $c = 0.0218$ for downflow and 0.0201 for upflow. Significant improvement in predicting heat transfer and an explanation of the variation of heat transfer with the wall to bulk temperature ratio (T_w/T_b) can be obtained if the bulk Prandtl number is replaced by one averaged harmonically over the range T_w to T_b. The upflow temperature profiles show buoyancy-induced peaks many of which occur at temperatures much higher than T_{pc}. The peaks can be quite well predicted by $Gr/Re^{2.7} > 2.4 \times 10^{-5}$, a criterion suggested by Hall's model of buoyancy-induced heat-transfer degradation.

NOMENCLATURE

- c, Dittus–Boelter coefficient, $Nu/(Re^{0.8}Pr^{0.4})$;
- C_p, specific heat at constant pressure;
- D, test section internal diameter;
- G, average mass flow-rate per unit area, $4\dot{m}/\pi D^2$;
- g, acceleration due to gravity;
- Gr, Grashof number $\rho_b(\rho_b - \rho_w)gD^3/\eta_b^2$;
- h, heat-transfer coefficient;
- h^*, reduced heat-transfer coefficient $hD^{0.2}/G^{0.8}$;
- k, thermal conductivity;
- k_A, thermal conductivity of test-section wall;
- L, test section length;
- $\dot{m}$, mass flow rate;
- Nu, Nusselt number hD/k;
- p, pressure;
- P_c, critical pressure, 2.27 bars;
- Pr, Prandtl number $C_p\eta/k$;
- Pr_{pc}, Pr at T_{pc};
- $\overline{Pr}$, averaged Prandtl number;
- q, heat input per unit area;
- Re, Reynolds number GD/η;
- s.d., standard deviation;
- t, test-section wall thickness;
- T, temperature;
- T_{pc}, pseudo-critical temperature;
- T_c, critical temperature, 5.20 K;
- T_o, outlet fluid temperature;
- T_i, inlet fluid temperature;
- T_w, inner wall temperature;
- T_b, bulk fluid temperature as determined from heat-balance equation;
- x, distance from start of heater;
- ρ, density;
- η, viscosity.

Subscripts

- b, parameter evaluated at T_b;
- w, parameter evaluated at T_w.

1. INTRODUCTION

SUPERCRITICAL heat transfer has received much attention in recent years and there are several review articles [1–3]. The main problem has always been regarded as the large property variations occurring near the critical point; these cause the breakdown of conventional correlations, which deal with property variation by using a film temperature or by including property-ratio terms of the type $(T_w/T_b)^n$, $(\eta_w/\eta_b)^n$, $(C_{p_w}/C_{p_b})^n$. However, more recently, the effect of buoyancy forces, particularly in upflow in larger pipes, has been recognised, and identified as the cause of the sharp deteriorations in heat transfer encountered under these conditions [1, 2, 4–11].

Heat transfer to supercritical helium is of importance in the cooling of superconducting machines, magnets and power transmission cables and there have been several previous measurements [12–14] but of these only the work of Giarratano *et al.* [14] and of Ogata and Sato [15] deal with comprehensive measurements. Both these experiments used narrow tubes, 1–2 mm i.d., so buoyancy effects were not important, and measured the wall temperature at only two points along the test section. Our test section was instrumented with 18 thermometers for upflow and 9 for downflow. The conditions covered in the present work correspond with those likely to be encountered in a superconducting cable; they cover a considerably wider range of p/p_c and T/T_c than in experiments exclusively concerned with near-critical heat transfer.

2. EXPERIMENTAL ARRANGEMENT

Figure 1 shows the helium flow loop installed in its cryostat [25]. A centrifugal pump circulates the helium through the vacuum-jacketed test section, then through a turbine flowmeter (previously calibrated on helium) to a bypass valve, which allows some of the flow to pass directly back to the pump while the remainder

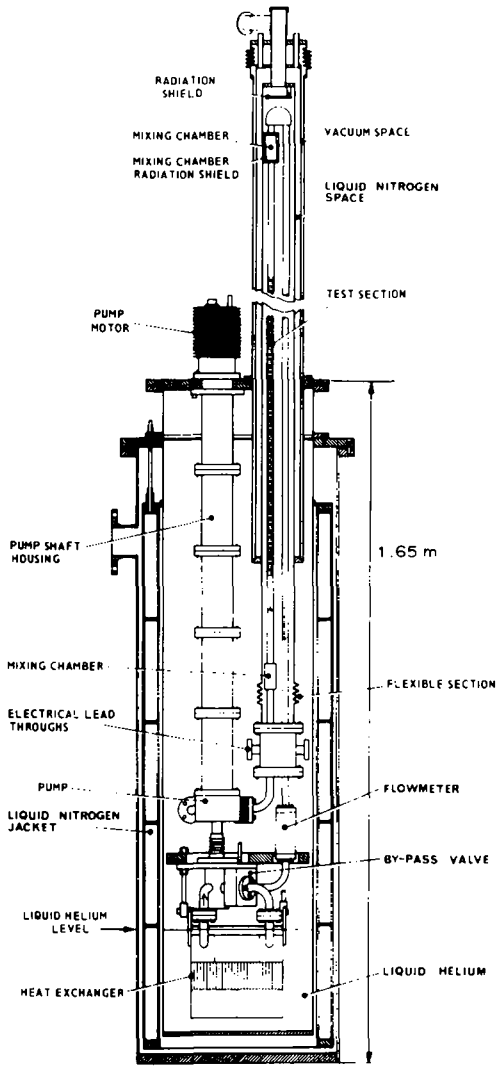

FIG. 1. The cryostat and flow loop.

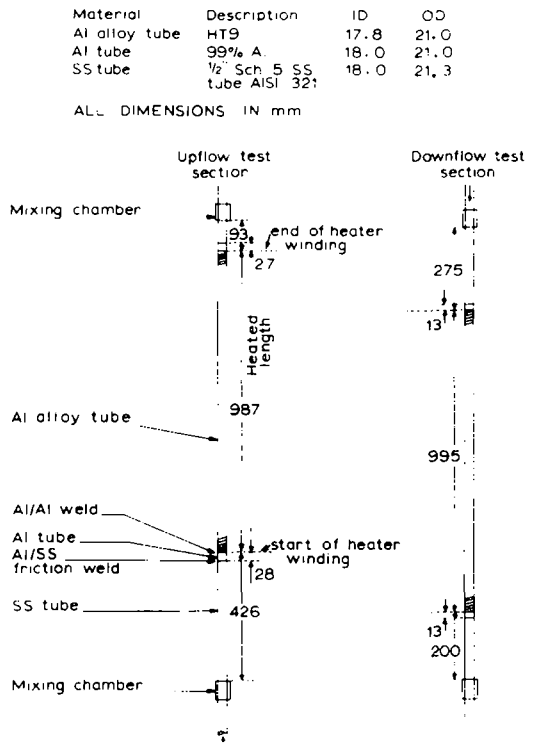

FIG. 2. Details of the test sections.

passes through a heat exchanger immersed in liquid helium at its atmospheric-pressure boiling point of 4.2 K. The figure shows the arrangement for upflow measurements, for downflow the test section is in the other leg of the inverted U section of the loop. The bypass valve can be controlled from outside the cryostat and its setting in conjunction with the heat input to the test section determines the bulk fluid temperature at the entrance to the test section. The flow velocity is typically 1 m/s which gives a loop transit time of order 5 s. The heat exchanger was large enough to maintain a fluid inlet temperature of ~ 4.5 K over the full range of heat input and flow conditions.

Figure 2 gives details of the test sections. The heated section consists of HT 9 aluminium alloy drawn tube with a 28 s.w.g. Eureka heater wire wound onto it in a spiral groove of 2 mm pitch. The mixing chambers contain flow diffusers and the bulk fluid temperature is monitored at the mixing chambers by calibrated germanium resistance thermometers. The wall temperature of the test section is measured by carbon resistance thermometers [16]. These needed to be recalibrated every run against the germanium thermometers by running the pump with no heat input to the test section. A small correction for the temperature gradient across the wall was applied to the outer wall temperatures to obtain the inner wall temperatures. We estimate that temperature measurement was accurate to within 10 mK. The readings of the inlet and outlet thermometers with no heat input agreed to within 5 mK.

For various reasons mainly concerned with avoiding excessive boil-off from the helium bath it was not possible to maintain constant test-section inlet conditions whilst varying the heat input, and our measurement procedure was to set the bypass valve and pump speed and then to stabilize the loop at a series of increasing temperatures by adjusting the heat input.

Our results thus consist of some hundreds of wall temperature profiles taken at fairly random values of inlet temperature, pressure, flow rate, and heat input. The variation of T_b along the test section was calculated from the inlet-temperature and heat-input assuming a linear increase of enthalpy along the test section (the pressure drop along the test section was negligible). Mass flow-rate was obtained from the inlet and outlet bulk fluid temperatures using a heat balance; we preferred this to the value obtained from the volume flow-rate indication of the turbine flowmeter because of some uncertainty in the temperature and thus density of the fluid passing through the flowmeter, which is outside the vacuum insulating jacket. The two values of mass flow-rate anyway agreed to within 5% on average.

The various helium thermodynamic properties needed in the analysis were determined from a com-

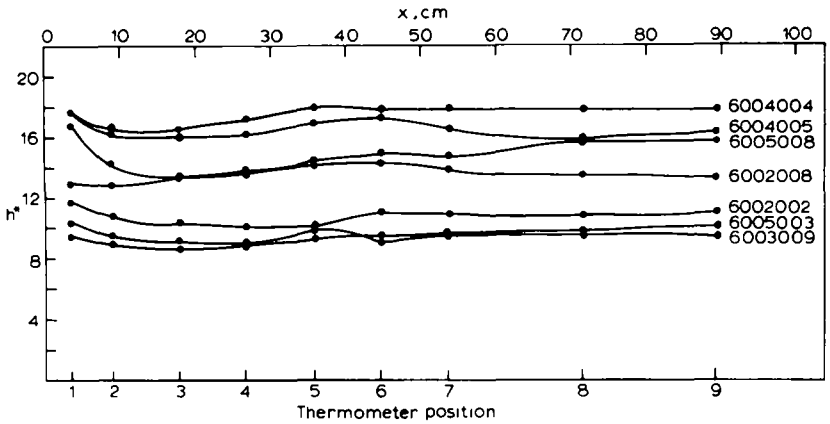

FIG. 3. Variation of h^* ($= hD^{0.2}/G^{0.8}$) along the test section for a selection of downflow scans. (Table 1 gives details of all scans shown in the figures.)

puter code of McCarty [17], viscosity from an equation of Steward and Wallace [19] and thermal conductivity from an equation of Roder [18]. These properties are estimated to be accurate to ~2% except for thermal conductivity, for which, due to lack of data, Roder estimates an accuracy of only 20%. However, recent preliminary measurements of Acton (private communication) indicate that Roder's correlation is actually accurate to better than 10%.

The main source of error in the heat-transfer measurements is the measurement of temperature. This leads to an error of ~3% in h from errors in $T_w - T_b$. There is also an error of ~3% in flow rate resulting from errors in $T_o - T_i$. Any sharp changes in T_w along the test section (e.g. a buoyancy peak) will have been affected by conduction along the tube wall. This means that detail in the temperature profile with a scale of less than $(k_A t/h)^{1/2}$ where t is the wall thickness and k_A its thermal conductivity will not be fully resolved. This characteristic length is typically 10 mm for our measurements.

3. DOWNFLOW RESULTS

The heat-transfer coefficient $h[= q/(T_w - T_b)]$ varied only slightly with x/D, typically by ±5% (see Fig. 3). The first thermometer at $x/D = 2$ always showed slight enhancement, due partly to the usual entrance effect and partly to heat conduction along the wall to the unheated part of the loop, but for higher x/D no systematic variation could be discerned and h settled to a steady value beyond $x/D = 30$. We therefore chose to analyze only the data for the thermometer at $x/D = 40$. These data comprised 161 points with p, q, T_b, and Re spread over the range quoted earlier but with 70% of the points having $T_b < 7$ K. The data were first fitted to the standard Dittus–Boelter correlation

$$Nu = cRe_b^{0.8}Pr_b^{0.4} \quad (1)$$

giving $c = 0.0218$ and a standard deviation of 11.2%. Allowing the exponents to vary gave

$$Nu = 0.0689Re_b^{0.711}Pr_b^{0.44} \quad (2)$$

improving the fit to 9.1%. Figure 4 shows a comparison of the data with this correlation. The $Re^{0.711}$ rather than $Re^{0.8}$ dependence is unexpected; it is not attributable to near-critical property variation (equation 1 is strictly a constant-property correlation) since removing the near-critical data did not change the exponent.

Equation (1) is often modified for variable-property fluids by including a $(T_w/T_b)^n$ factor. This did not improve the fit to our data as a whole, but, if the two sub-groups of data defined by $T_b < T_w < T_{pc}$ and $T_{pc} < T_b < T_w$ were correlated separately using such a term, the former group gave a best fit value of n of 0.4 while the latter gave $n = -0.7$. This can be understood if one postulates that Pr_b in equation (1) should be

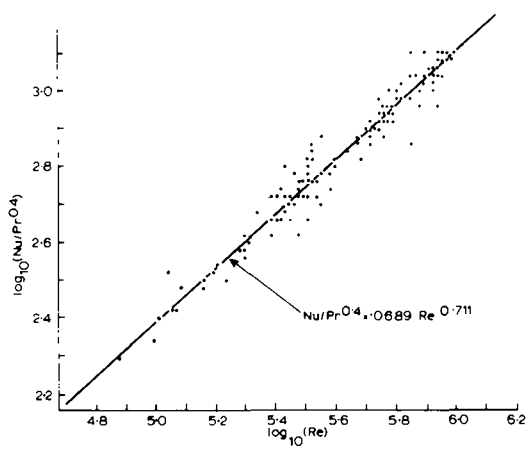

FIG. 4. Variation of $\log_{10}(Nu/Pr^{0.4})$ with $\log_{10}(Re)$ for the downflow data.

replaced by a Prandtl number averaged over the range T_w to T_b ($\overline{Pr}$). Because Pr has a maximum at T_{pc} $\overline{Pr} > Pr_b$ for $T < T_{pc}$ and $\overline{Pr} < Pr_b$ for $T > T_{pc}$. The prediction of equation (1) is therefore too low for $T < T_{pc}$ and too high for $T > T_{pc}$ and the $(T_w/T_b)^n$ exponent thus needs to be $+ve$ and $-ve$ respectively to compensate. A correlation using an averaged Prandtl number was therefore tested and proved very successful with

$$Nu = 0.0931Re_b^{0.687}\overline{Pr}^{0.53} \quad (3)$$

representing the data with a standard deviation of 6.4%, not much higher than the expected experimental

Table 1. Details of scans shown in the figures

	p (bar)	q (W m^{-2})	$\dot{m}$ (kg s^{-1})	T_w at $x/D = 40$	T_b at $x/D = 40$	T_i	T_o
Downflow							
6002002	5.79	306	0.0167	5.79	5.36	5.22	5.41
6002008	11.26	1254	0.0055	18.04	14.60	13.21	15.18
6003009	7.61	167	0.0409	5.13	5.00	4.96	5.02
6004004	6.44	721	0.0097	7.91	6.96	6.68	7.06
6004005	7.17	675	0.0076	9.19	7.98	7.63	8.12
6005003	5.66	634	0.0170	5.65	4.68	4.29	4.81
6005008	4.94	2576	0.0142	8.56	5.70	4.35	6.02
Upflow							
6502007	6.23	318	0.0126				
6502008	6.17	512	0.0123				
6502009	6.83	524	0.0095				
6502010	8.44	522	0.0067				
6502011	10.28	648	0.0057				
6502012	12.16	897	0.0046	17.37	14.14	12.97	14.63
6502013	14.09	1082	0.0047	20.41	16.39	14.98	16.98
6506007	8.06	1266	0.0042	19.91	14.50	12.57	15.29
6601006	10.97	935	0.0041	19.62	15.80	14.35	16.39
6601019	6.14	876	0.0037	15.61	11.50	10.08	12.11
6602005	3.87	246	0.0067	6.91	6.43	6.32	6.46
6602009	6.06	1760	0.0155	11.18	7.67	7.25	7.85
6603002	3.40	832	0.0121	6.05	4.84	4.26	5.02
6603004	2.33	353	0.0249	4.93	4.48	4.37	4.53
6603006	2.35	1514	0.0235	6.10	4.95	4.58	5.05
6604008	8.08	1026	0.0040	17.84	13.43	11.85	14.10
6605006	4.49	534	0.0028	13.06	9.94	8.81	10.43
6605007	4.60	774	0.0026	17.80	12.53	10.62	13.32

Table 2. Upflow correlations (216 points)

Correlation number	Correlation equation	C_1	C_2	C_3	C_4	Standard deviation (%)
U_1	$Nu = C_1 Re^{0.8} Pr^{0.4}$	0.0201				12.6
U_2	$Nu = C_1 Re^{C_2} Pr^{C_3}$	0.0253	0.782	0.39		12.3
U_3	$Nu = C_1 Re^{C_2} \overline{Pr}^{C_3}$	0.0447	0.735	0.49		9.5
U_4	$Nu = C_1 Re^{C_2} \overline{Pr}^{C_3} (T_w/T_b)^{C_4}$	0.0602	0.718	0.50	−0.48	8.5

error of ±4%. The $\overline{Pr}$ used was a simplified harmonic average over the range T_w to T_b

$$1/\overline{Pr} = (1/Pr_w + 1/Pr_b)/2 \qquad T_w < T_{pc} \text{ or } T_b > T_{pc}$$

$$1/\overline{Pr} = [(1/Pr_b + 1/Pr_{pc})(T_{pc} - T_b) + (1/Pr_{pc} + 1/Pr_w)(T_w - T_{pc})]/2(T_w - T_b) \qquad T_b < T_{pc} < T_w. \quad (4)$$

This gave the best fit of several averaging methods tested and was suggested by analogy with thermal conductances which add harmonically.

We examined the data for any deviations from equation (3) but were unable to find any which could not be attributed to experimental errors. Obviously equation (3) is not a perfect representation of the heat-transfer function but the experimental errors and the wide spacing of experimental points in the 4-dimensional space T_b, q, G, p do not allow further systematic deviations to be discovered.

4. UPFLOW RESULTS

The heat-transfer coefficient showed greater variation with x/D than for downflow (Fig. 5) and, in particular, buoyancy-induced reductions of h (equivalent to peaks in T_w) occurred in about 25% of the profiles. This is discussed in the next section. Apart from these no systematic trends in the x/D variation were evident and we again analysed a single thermometer position, $x/D = 45$. Details of some of the correlations tested are given in Table 2. The use of $\overline{Pr}$ was again successful but, in contrast to the downflow data, a $(T_w/T_b)^n$ factor did improve the fit further. The data show more scatter from the best correlation than for downflow but again no systematic deviations from it could be discovered. The upflow data fall ~20% below the downflow data at $Re = 10^5$ but downflow and upflow heat transfer are equal at $Re = 10^6$.

Both the upflow and downflow data were checked for unwanted correlations between the independent variables Re, Pr and (T_w/T_b) but the highest correlation coefficient was 0.3 which would not be expected to affect the correlation equations.

5. BUOYANCY EFFECTS

5.1. *Wall-temperature peaks*

These peaks occurred only for upflow which strongly suggests that some buoyancy effect of the type suggested by Hall *et al.* [2] is responsible. Forty-five of the 184

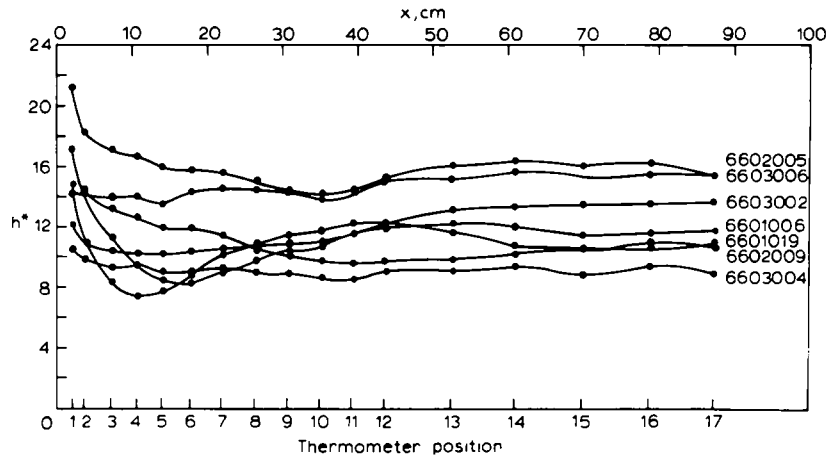

FIG. 5. Variation of h^* along the test section for a selection of upflow scans.

upflow profiles examined showed a peak and they almost all coincided with low flow-rates (< 0.01 kg/s). The peaks always occurred between $x/D = 5$ and $x/D = 20$ and in general the higher the heat input the sharper and higher the peak and the nearer the start of the test section it occurred. Peaks were not predominantly associated with temperatures close to T_{pc} as has been usual in previous experiments [4, 6, 11, 20–21]. Figure 6 shows the development of peaks as heat input increases with successive scans. Peaks have not previously been observed with helium, simply because pipe diameters have been too small, but they are frequently observed with supercritical CO_2 [23, 5, 6] and supercritical water [4, 20, 22] where they occur only for upflow and usually with T_b close to or below T_{pc}. They have also been observed with non-supercritical water [24]. Hall's explanation of the effect is that with variable- property fluids and particularly supercritical fluids a buoyant low-density layer occurs near the wall. For upflow this reduces the shear stress over the turbulent core and hence the rate of turbulence production and heat transfer. For upflow with constant heat flux the heat-transfer degradation is self reinforcing —hence the occurrence of wall temperature peaks. For downflow buoyancy improves heat transfer and is therefore self-stabilizing and no peaks occur. Hall assumes that buoyancy is significant if the shear stress is reduced by $> 10\%$ at $y^+ = 30$ (turbulence production is normally at a maximum between $y^+ = 10$ and $y^+ = 30$) and shows that this is equivalent to

$$Gr/Re^{2.7} > 1.2 \times 10^{-5} \tag{5}$$

where Gr is the Grashof number:

$$Gr = \frac{\rho_b(\rho_b - \rho_w)gD^3}{\eta_b^2}. \tag{6}$$

The detailed mechanism of peaking is not yet understood so it is not clear whether the condition that buoyancy forces are significant is equivalent to a condition for peaks to occur, but this assumption seems reasonable as a first step. In Fig. 7 peaked and unpeaked scans are plotted in the Re–Gr plane showing that equation (7) is satisfied by all but three of the

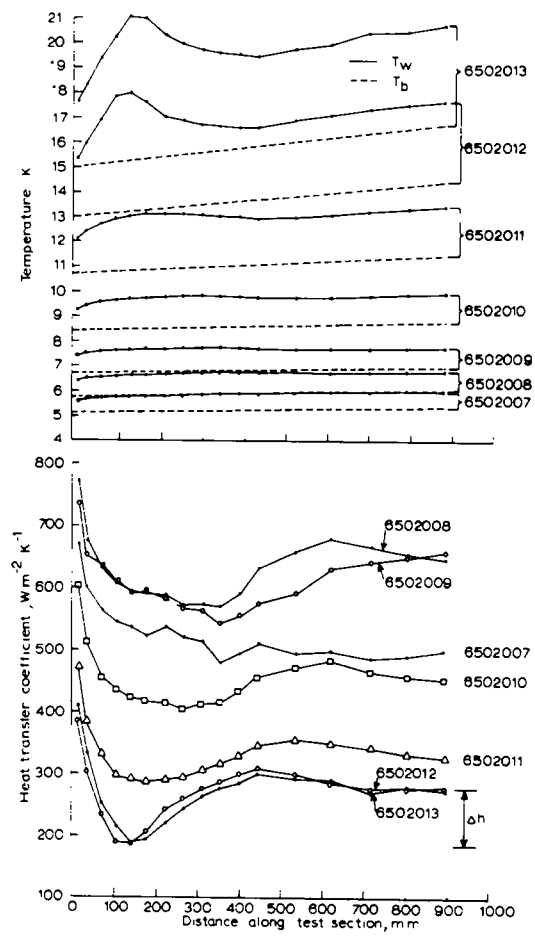

FIG. 6. Heat transfer and temperature profiles for a sequence of upflow scans showing the development of a wall temperature peak.

peaked scans and that the condition can be made more restrictive:

$$Gr/Re^{2.7} > 2.4 \times 10^{-5} \tag{7}$$

without excluding any more peaked scans. The value of the constant in equation (5) is anyway arbitrary since it depends directly on what percentage reduction in shear stress is assumed to be significant. Equation (7)

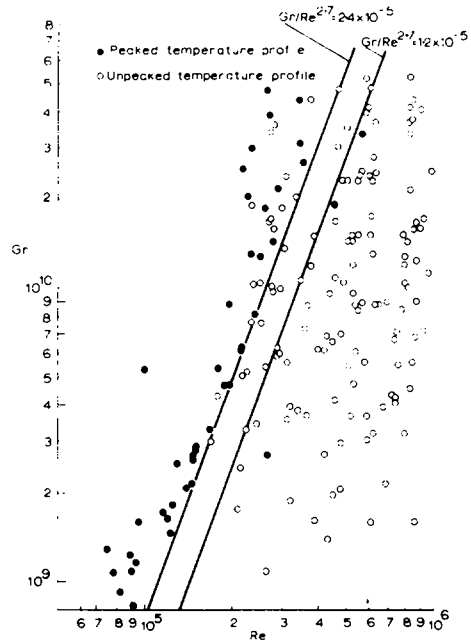

FIG. 7. *Gr–Re* scatter plot showing the influence of $Gr/Re^{2.7}$ on peaking.

appears from Fig. 7 to be a necessary but not sufficient condition for the occurrence of temperature peaks, but investigation of those scans which satisfy equation (7) and yet have no peak shows that either they lie close to the critical point where property values and hence *Re* and *Gr* are most liable to error, or they are scans for which the decision is borderline as to whether or not a peak is present.

We noticed that whilst the majority of peaks were quite small ($\Delta h/h \approx 0.05$, where the meaning of Δh is shown in Fig. 6), there was a group of much larger peaks with $\Delta h/h \approx 0.28$, all having very similar shape (see Fig. 8). These large peaks all occurred for $T_w > T_b > 10$ K and at high values of $Gr\,Re^{2.7}$. It is not clear why there were no peaks of intermediate size or why the peaks should be so similar in shape. Large peaks with $\Delta h/h > 0.25$ also occurred when $T_w > T_{pc} > T_b$ but they were much sharper, as might be expected from the more-rapid property variations near T_{pc}.

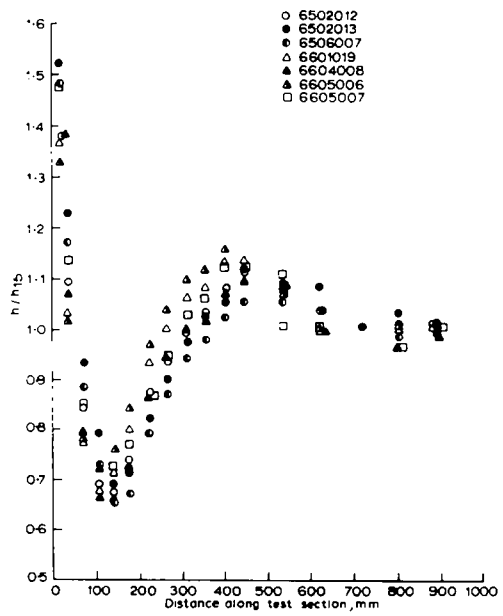

FIG. 8. Normalised *h* profiles for the group of scans showing large peaks. Values plotted are h/h_{15} where h_{15} is the value of *h* at thermometer position 15 ($x = 703$ mm, $x/D = 40$).

5.2. *Other effects*

There are two other indications of the effect of buoyancy on the results. The first is the difference between upflow and downflow heat transfer at low *Re*. This can be explained as a buoyancy effect because low-flowrate upflow heat transfer would be expected to be most degraded by buoyancy forces. Secondly the negative exponent of the $(T_w - T_b)$ term in upflow correlation U4 could be due to buoyancy because, in upflow, reduction of heat transfer by buoyancy would be greater for high values of $(T_w - T_b)$.

6. CONCLUSIONS

Our results show that over the range of conditions covered in this work supercritical helium is a well-behaved heat-transfer fluid: even an unmodified Dittus Boelter equation has a predictive accuracy of 10–20% which is sufficient for most design purposes. The major deviations from the Dittus–Boelter equation can be accommodated by using a Prandtl number averaged reciprocally over the range T_w to T_b, i.e. $[\overline{Pr(T)^{-1}}]^{-1}$; this achieved an accuracy of 6% with the downflow data.

The upflow data displays wall-temperature peaks similar to ones previously seen with supercritical CO_2 and water. The peaks, and other effects, are well explained by Hall's model of buoyancy-induced heat-transfer degradation and we find that peaks occur when $Gr/Re^{2.7} > 2.4 \times 10^{-5}$. Many peaks occurred well away from the critical region showing that these buoyancy peaks are not an exclusively supercritical phenomenon.

Acknowledgements - We thank M. Graves for help in preparing the test sections and Professor W. B. Hall, J. D. Jackson, J. A. Hitchcock and J. Lis for valuable discussions. The work was carried out at the Central Electricity Research Laboratories and is published by permission of the Central Electricity Generating Board.

REFERENCES

1. W. B. Hall, Heat transfer near the critical point, in *Advances in Heat Transfer*, Vol. 7. Academic Press, New York (1971).
2. W. B. Hall, J. D. Jackson and A. Watson, A review of forced convection heat transfer to fluids at supercritical pressures, *Proc. Instn Mech. Engrs* **182**, Part 3I, 10–22 (1968).
3. R. C. Hendricks, R. J. Simoneau and R. V. Smith, Survey of heat transfer to near critical fluids, NASA Technical Memorandum NASA TMX-52612 (1969).
4. M. E. Shitsman, Temperature conditions in tubes at supercritical pressures, *Teploenergetika* **15**(5), 57–61 (1968).

5. K. O. J. Evans-Lutterodt, Forced convection heat transfer to carbon dioxide at near critical pressure conditions, Ph.D. Thesis, Manchester University (1970).
6. R. S. Weinberg, Experimental and theoretical study of buoyancy effects in forced convection to supercritical pressure carbon dioxide, Ph.D. Thesis, Manchester University (1972).
7. W. B. Hall and J. D. Jackson, Laminarization of a turbulent pipe flow by buoyancy forces, Am. Soc. Mech. Engrs. Paper No. 69-HT-55 (1969).
8. D. A. Labuntsov, Some questions of convective heat transfer in the supercritical region, *Teploenergetika* **19**(3), 69–72 (1972).
9. H. Tanaka, A. Tsuge, M. Hirata and N. Nishiwaki, Effects of buoyancy and of acceleration owing to thermal expansion on forced turbulent convection in vertical circular tubes—criteria of the effects, velocity and temperature profiles and reverse transition from turbulent to laminar flow, *Int. J. Heat Mass Transfer* **16**, 1267–1288 (1973).
10. H. Tanaka, N. Nishiwaki, M. Hirata and A. Tsuge, Forced convection heat transfer to fluid near critical point flowing in circular tube, *Int. J. Heat Mass Transfer* **14**, 739–750 (1970).
11. P. J. Bourke, D. J. Pulling, L. E. Gill and W. H. Denton, Forced convective heat transfer to turbulent carbon dioxide in the supercritical region, *Int. J. Heat Mass Transfer* **13**, 1339–1348 (1970).
12. R. D. Hay, Experimental data from a closed loop supercritical helium heat transfer system, Paper B-6, Cryogenic Engineering Conference (1969).
13. C. Johannes, Studies of forced convection heat transfer to helium–I, in *Advances in Cryogenic Engineering*, Vol. 17, pp. 352–360. Plenum Press, New York (1972).
14. P. J. Giarratano, V. D. Arp and R. V. Smith, Forced convection heat-transfer to supercritical helium, *Cryogenics* **11**, 385–393 (1972).
15. H. Ogata and S. Sato, Forced convection heat transfer to supercritical helium (in Japanese), *Teion Kogaku* (Cryogenic Engineering) **7**, 20–28 (1972); English translation, C.E. Trans. 6126, CEGB, Sudbury House, London.
16. P. Lindenfeld, Carbon and semiconductor thermometers for low temperatures, in *Temperature*, edited by C. M. Herzfelt, Vol. 3, Part I, pp. 399–405. Reinhold, Reading, MA (1962).
17. R. D. McCarty, New equation of state, in NBS Report 10573, Helium Heat Transfer (1972).
18. H. M. Roder, The thermal conductivity of helium I, in NBS Report 10703, Helium Heat Transfer (1971).
19. W. G. Steward and G. H. Wallace, Helium^4 viscosity measurements, NBS Report 10704 (1971).
20. M. E. Shitsman, Impairment of the heat transmission at supercritical pressures, *Teplofiz. Vysok. Temper.* **1**(2), 237–244 (1963).
21. Y. V. Vikrev, Y. D. Barulin and A. S. Kon'kov, A study of heat transfer in vertical tubes at supercritical pressures, *Teploenergetika* **14**(9), 80–82 (1967).
22. K. Yamagata, K. Nishikawa, S. Hasegawa, T. Fujii and S. Yoshida, Forced convective heat transfer to supercritical water flowing in tubes, *Int. J. Heat Mass Transfer* **15**, 2575–2593 (1972).
23. H. Tanaka, N. Nishiwaki and M. Hirata, Turbulent heat transfer to supercritical pressure carbon dioxide, *Proc. J.S.M.E. Semi-International Symposium, Tokyo, Heat Mass Transfer*, Vol. 2, pp. 127–134. J.S.M.E., Tokyo (1967).
24. D. B. R. Kenning, R. A. W. Shock and J. Y. M. Poon, Local reductions in heat transfer due to buoyancy effects in upward turbulent flow, Paper NC4.3 5th International Heat Transfer Conference, Tokyo (1974).
25. D. N. H. Cairns and D. J. Brassington, A pumped supercritical helium flow loop for heat transfer studies, *Cryogenics* **16**(8), 465–468 (1976).

MESURE DE CONVECTION THERMIQUE FORCEE DANS L'HELIUM

Résumé—On a mesuré le coefficient de convection forcée dans l'hélium supercritique s'écoulant vers le haut ou vers le bas, dans un tube vertical de 18 mm de diamètre intérieur. Les conditions correspondent aux domaines 4,4–15 K et 2,2–14 bar, avec des densités de flux atteignant 2500 W/m^2 et des nombres de Reynolds entre 5×10^4 et 10^6. Les résultats peuvent se représenter, avec une déviation standard $\sim 12\%$, par $Nu = cRe^{0,8}Pr^{0,4}$, où $c = 0{,}0218$ pour l'écoulement descendant et 0,0201 pour l'ascendant. Une amélioration significative dans la précision du transfert et une explication de la variation du transfert thermique, en fonction du rapport (T_w/T_b) des températures de la paroi et du fluide, peuvent être obtenues si le nombre de Prandtl moyen est remplacé par une moyenne harmonique de T_w et T_b. Les profils ascendants de température montrent des pics induits par les forces d'Archimède, pics dont plusieurs se produisent à des températures beaucoup plus grande que T_{pc}. Les pics peuvent être correctement prédits par $Gr/Re^{2,7} > 2{,}4 \times 10^{-5}$, critère suggéré par le modèle de Hall sur la dégradation du transfert thermique qui induit l'effet d'Archimède.

MESSUNG DES WÄRMEÜBERGANGS AN ÜBERKRITISCHES HELIUM BEI ERZWUNGENER KONVEKTION

Zusammenfassung—Es wurde der Wärmeübergangskoeffizient an überkritisches Helium, das entweder auf- oder abwärts in einem vertikalen Rohr mit 18 mm Innendurchmesser strömt, gemessen. Die Messungen wurden bei Temperaturen von 4,4 K–15 K, Drücken von 2,2 bar bis 14 bar, Wärmestromdichten bis 2500 W/m^2 und Reynolds-Zahlen von 5×10^4 bis 10^6 durchgeführt. Mit einer mittleren Abweichung von *ca.* 12% können die Ergebnisse durch die Formel $Nu = c \cdot Re^{0,8} \cdot Pr^{0,4}$ wiedergegeben werden, wobei für die Abwärtsströmung $c = 0{,}0218$ und für die Aufwärtsströmung $c = 0{,}0201$ einzusetzen ist. Setzt man statt der mittleren Prandtl-Zahl des Fluids eine über dem Bereich von T_w/T_b harmonisch gemittelte Prandtl-Zahl ein, dann kann die Vorausberechnung des Wärmeübergangs bedeutend verbessert werden und die Veränderung des Wärmeübergangs mit dem Temperaturverhältnis (T_w/T_b) zwischen Wand und Fluid erklärt werden. Die Temperaturprofile bei Aufwärtsströmung zeigen auftriebsbedingte Spitzen, von denen viele weit höhere Temperaturen als T_{pc} aufweisen. Diese Spitzen können recht gut mit $Gr/Re^{2,7} > 2{,}4 \times 10^{-5}$ vorhergesagt werden, ein Kriterium, welches aus dem Modell von Hall für die Abschwächung des Wärmeübergangs infolge Auftriebs hervorgeht.

ПЕРЕНОС ТЕПЛА ПРИ ВЫНУЖДЕННОЙ КОНВЕКЦИИ К СВЕРХКРИТИЧЕСКОМУ ГЕЛИЮ

Аннотация — Измеряется коэффициент теплопереноса сверхкритического гелия, движущегося вверх и вниз по вертикальной трубе с внутренним диаметром 18 мм, при температуре 4,4–15К, давлении 2,2–14 бар, тепловых потоках до 2500 вт/м^2 и числах Рейнольдса в пределах от 5×10^4 до 10^6. Результаты можно представить со стандартными отклонениями $\sim 12\%$ в виде формулы $Nu = cRe^{0,8}Pr^{0,4}$, где $c = 0{,}0218$ для нисходящего и 0,0201 для восходящего потока. Можно добиться значительного уточнения зависимости теплопереноса за счет учета фактора (T_w/T_b) путем замены основного числа Прандтля другим, гармонически осредненным в пределах от T_w до T_b. Профили температуры восходящего потока создают максимальные значения коэффициентов теплопереноса, вызываемые подъемными силами, имеющими место при температурах намного выше, чем T_{pc}. Максимальные значения можно достаточно точно рассчитать по критерию $Gr/Re^{2,7} > 2{,}4 \times 10^{-5}$, предлагаемому моделью Холла для ослабления теплопереноса, вызываемого подъемными силами.